Electronic Supplementary Material (ESI) for Journal of Materials Chemistry A.
This journal is © The Royal Society of Chemistry 2017

Supporting Information

Cyclic Molecule Aerogels: A Robust Cyclodextrin Monolith with Hierarchically Porous Structures for Removal of Micropollutants from Water

*Jin Wang, Xuchun Wang, and Xuetong Zhang**

Suzhou Institute of Nano-Tech and Nano-Bionics, Chinese Academy of Sciences, Suzhou 215123, P. R. China

Correspondence author: zhangxtchina@yahoo.com

Experimental

Adsorption experiment

Batch experiments were carried out to investigate the adsorption performance of the aerogel to methyl orange, rhodamine B, and BPA, with dilute concentration of 0.1 mM. Normally, ca. 4 mg of aerogel were dispersed in 10 ml of the dye aqueous solution at room temperature (25 ^{o}C).

The amount of pollutant bound to the aerogel was determined by the following equation:

$$q_t = (C_0 - C_t) M_w V / m$$

where q_t (mg g^{-1}) is amount of pollutant adsorbed per g of sorbent at time t (min). C_0 (mmol L^{-1}) and C_t (mmol L^{-1}) are the initial and residue concentration of pollutant in the solution. M_w (g mol^{-1}) is the molar mass of the dye, V (ml) is the volume of the solution, and m (g) is the mass of sorbent.

In order to investigate the adsorption kinetic and isotherm, rhodamine B was used as the pollutant, and aerogel CD-TTI200 was used as sorbent. The temperature was set to 30 ^{0}C, and C_0 of 0.1 mM was used to study the adsorption kinetic.

The uptake rate of each adsorbent was best described by Ho and McKay's pseudo-second-order adsorption model, as expressed as the following:

$$t/q_t = 1/k_2 q_e^2 + t/q_e$$

where q_e and q_t are the adsorbate uptakes (mg/g) at equilibrium and time t (min), respectively, K_2 is the pseudo-second-order adsorption rate constant (g mg^{-1} min^{-1}).

In the adsorption isotherm study, Freundlich model was employed, the model can be expressed in the linear form as the following:

$$\ln q_e = \ln K_F + n^{-1} \ln C_e$$

where q_e and C_e are the equilibrium adsorption capacity (mg/g) and equilibrium concentration (mmol L^{-1}), respectively.

Figures of the Supporting Information

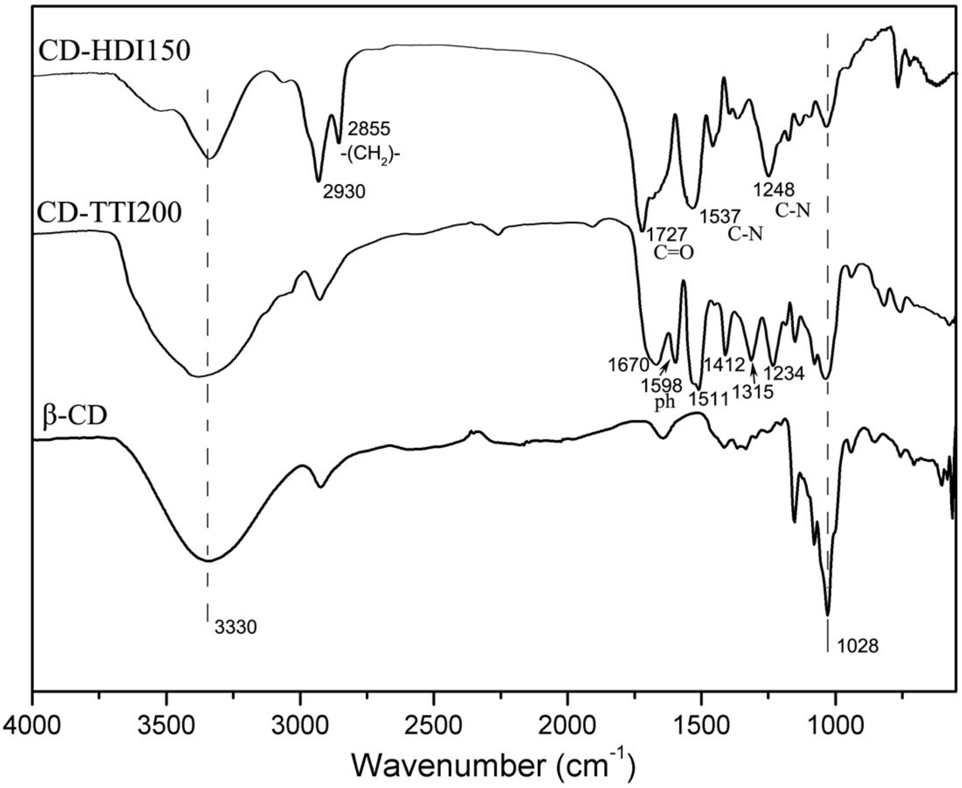

Figure S1. FTIR spectra of CD-HDI150, CD-TTI200 and β-CD.

Figure S1 show the FTIR spectra of CD-HDI150, CD-TTI200 and β-CD. The characteristic peaks of β-CD at 1028 and 3330 cm^{-1} are found in both the HDI and TTI cross-linked aerogels, demonstrating the present of β-CDs. Moreover, no peaks were found around 2500 cm^{-1} corresponding to the –NCO in the aerogels, while the peaks from urethane bonds (1727, 1537, and 1248 cm^{-1} for the HDI cross-linked aerogels; 1670, 1511,and 1234 cm^{-1} for the TTI cross-linked aerogels) were clearly identified. The results indicated that the β-CDs were successfully cross-linked by HDI or TTI at 80 ^{o}C in DMF without any catalyst.

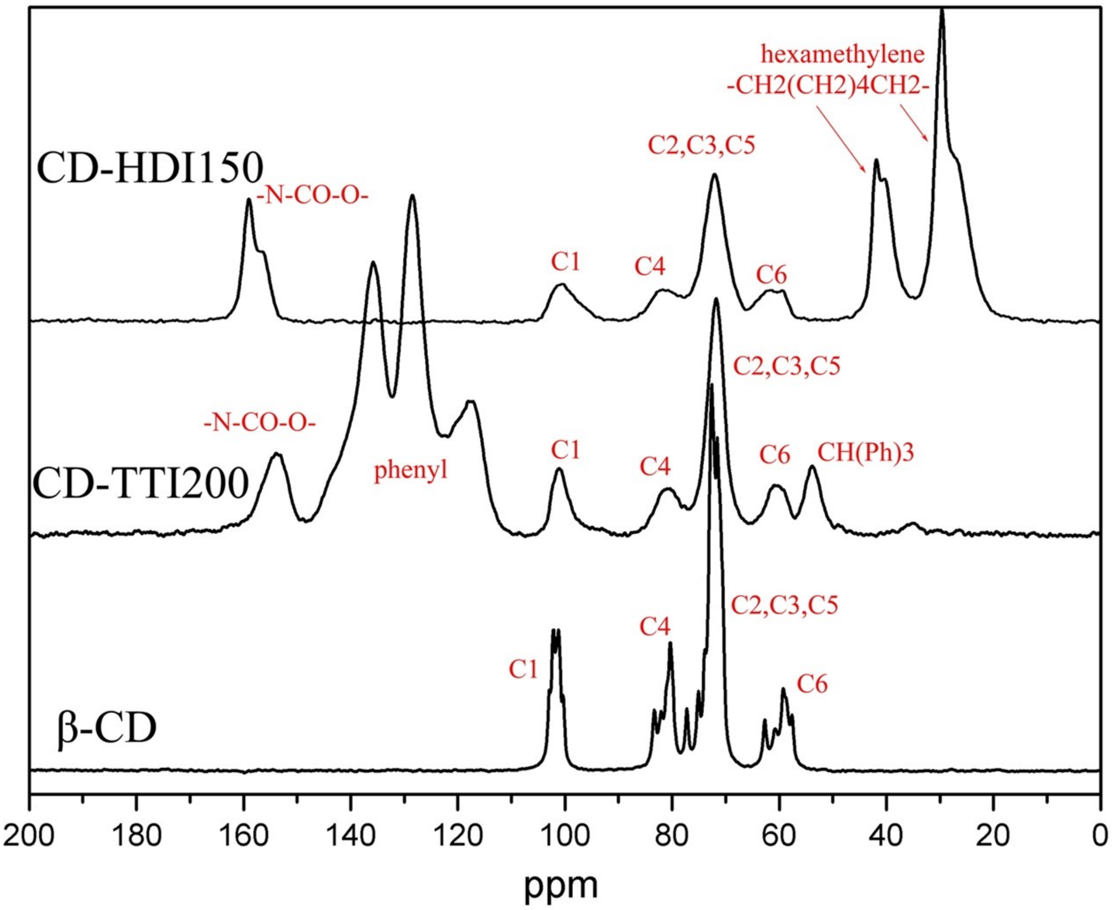

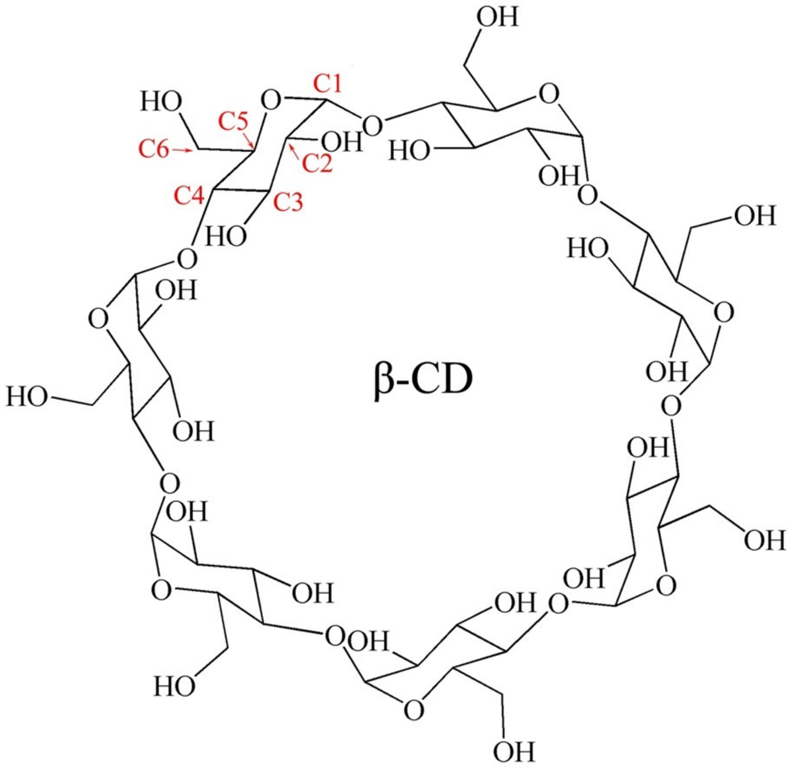

Figure S2. Solid-state ^{13}C CP/MAS NMR spectra of CD-HDI150, CD-TTI200 and β-CD.

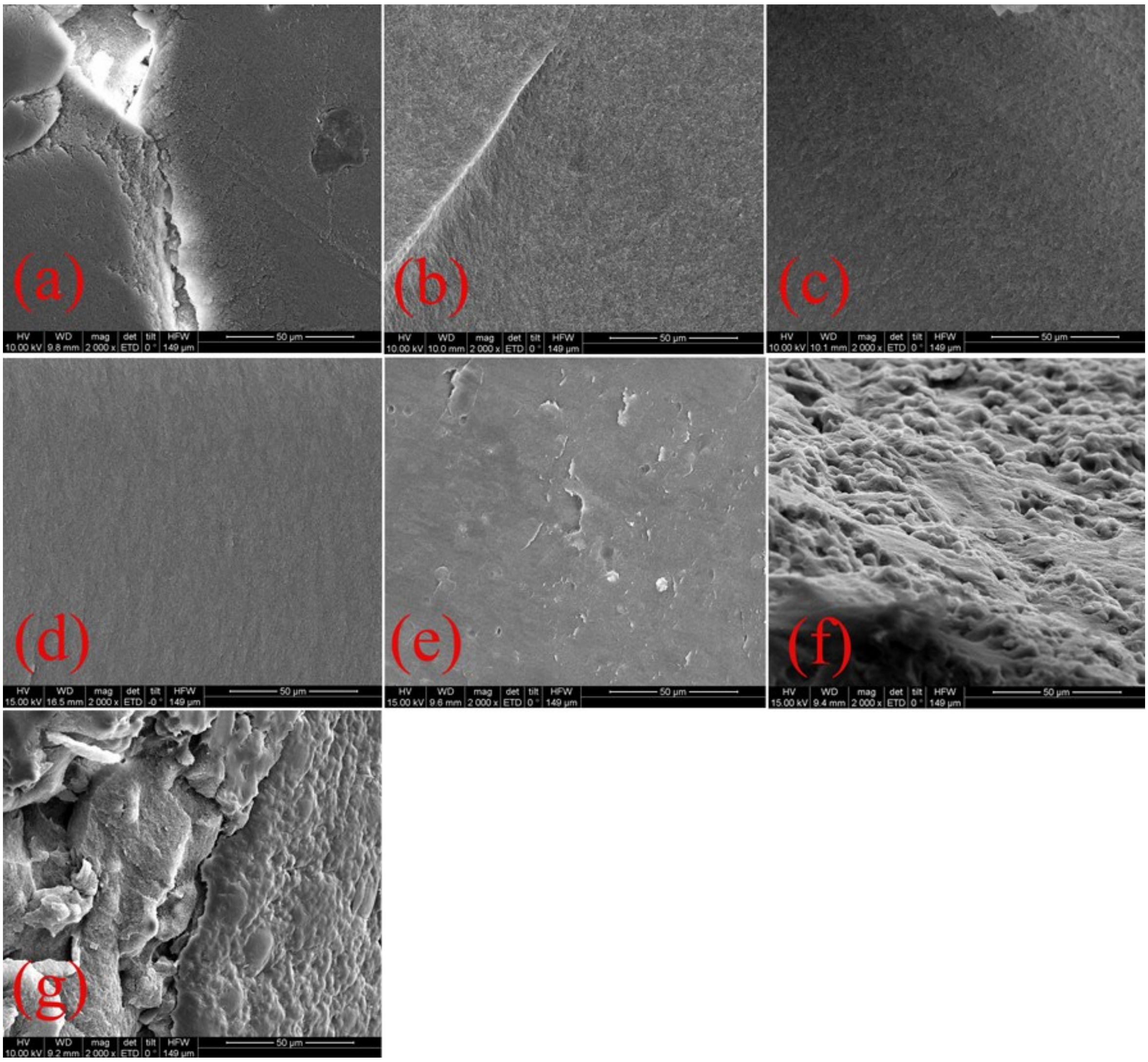

Figure S3. SEM images of CD-TTI100 (a), CD-TTI200(b), CD-TTI266(e), CD-TTI400(f), CD-HDI100(e), CD-HDI150(f), and CD-HDI200(g) with the scale bar of 50 μm.

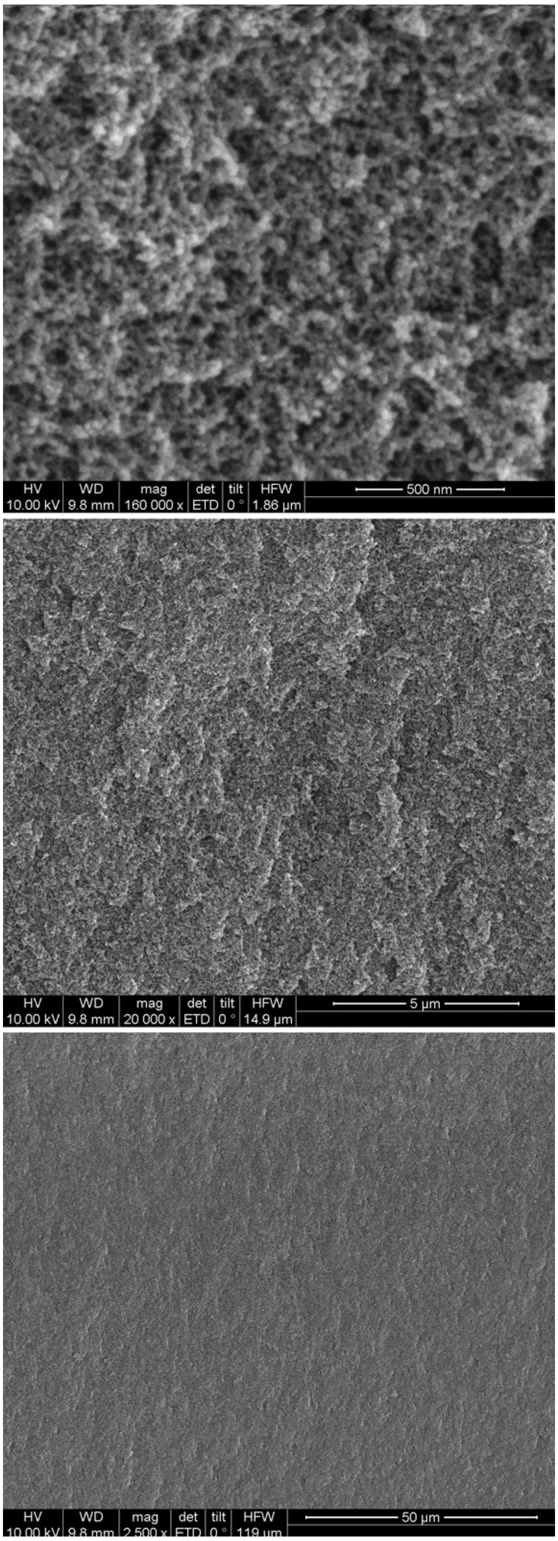

Figure S4. SEM images CD-TTI300 in difference scales: 500 nm, 5 µm, and 50 µm.

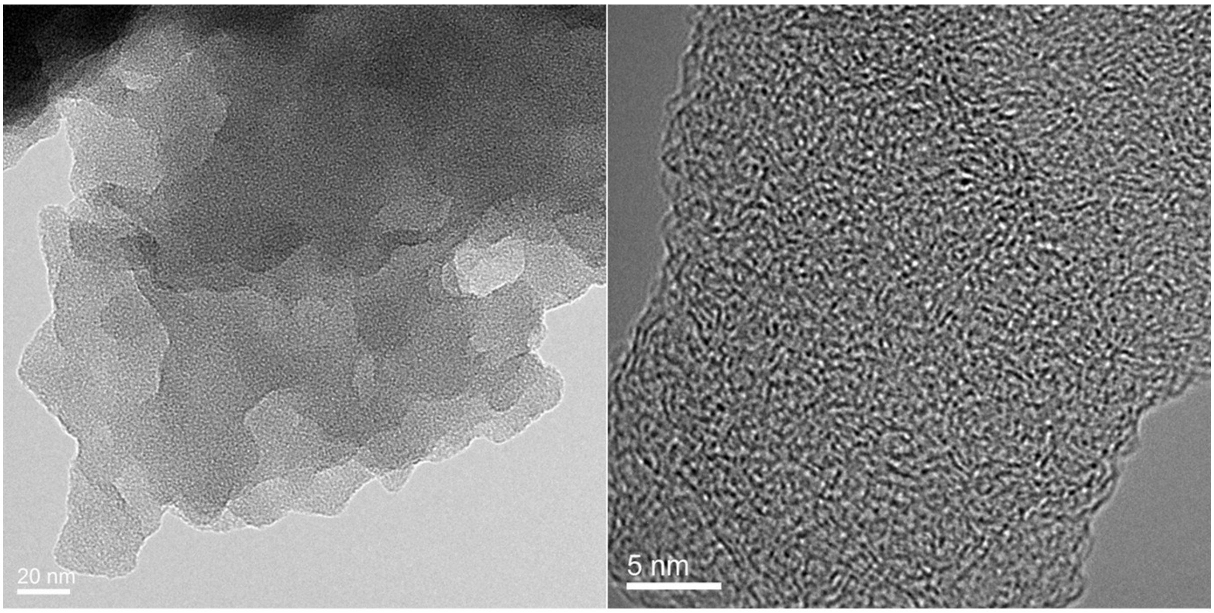

Figure S5. TEM images of xerogel from CD-TTI300.

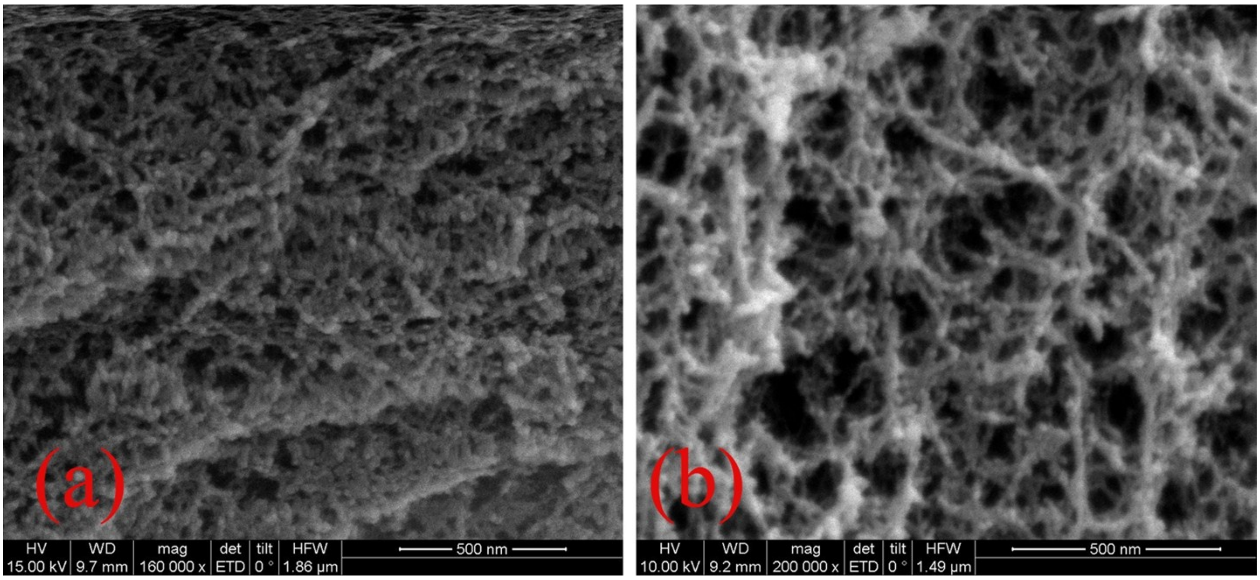

Figure S6. SEM images of CD-HDI100 (a) and CD-HDI200 with the scale bar of 500 nm.

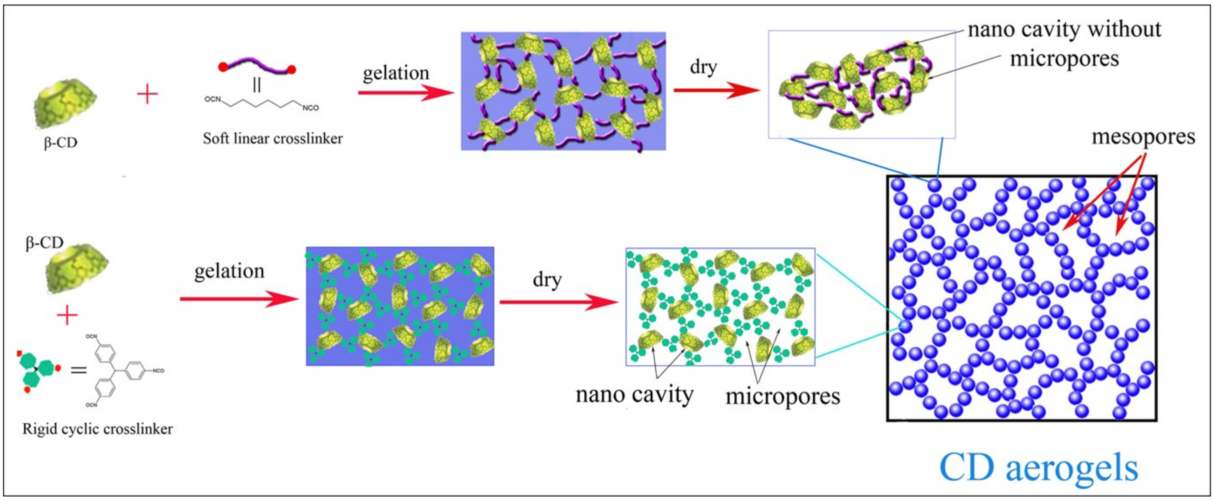

Figure S7. Proposed mechanism for the formation of nano cavities, micropores, and mesopores in the CD aerogels.

For the HDI cross-linked aerogels, the CDs may collapsed due to the soft nature of HDI, so there was no micropores in the HDI cross-linked aerogels as illustrated in Figure S6. However, for the TTI cross-linked aerogels, due to the rigidities of TTI and CD, the micropores formed between CD and TTI may preserved during SCLD. Therefore, there are both nano cavity and micropore in the TTI cross-linked aerogels. On the other hand, both the HDI and TTI cross-linked wet gels were formed by sol-gel process, therefore, phase separation induce the mesopores in the CD gelation networks as illustrated in Figure S6.

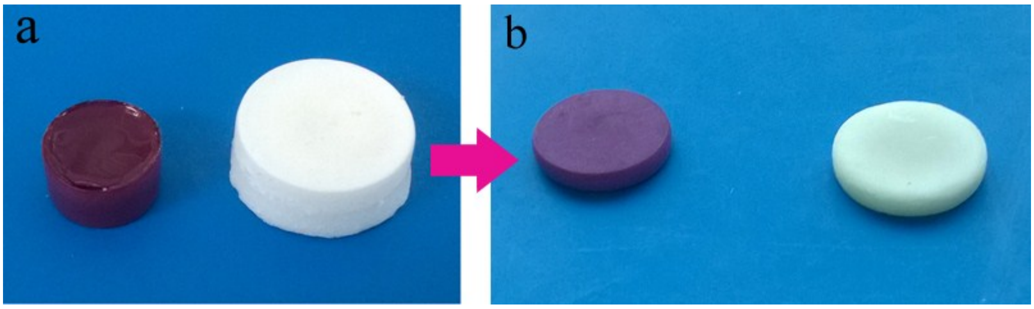

Figure S8. Photo images of CD aerogels before (a) and after compression (b): The purple one is CD-TTI266 (compression for 70%), and the white one is CD-HDI200 (compression for 60%).

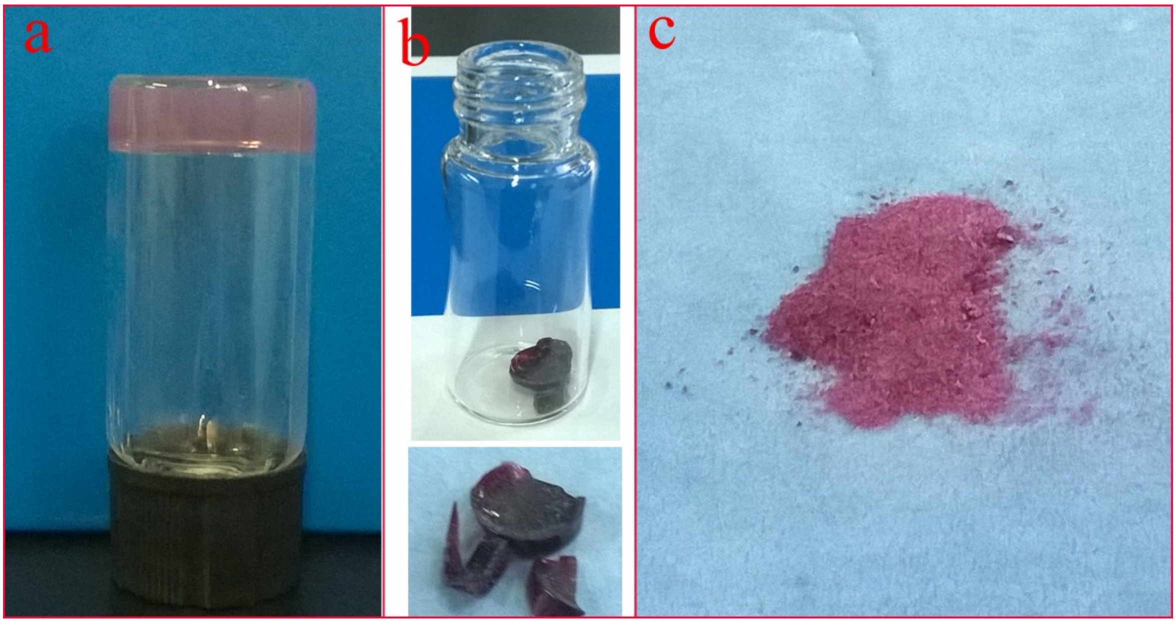

Figure S9. Photo images wet gel CD-TTI200 (a), the corresponding ambient pressure dried xerogel (b), and the crashed xerogel powders (c).

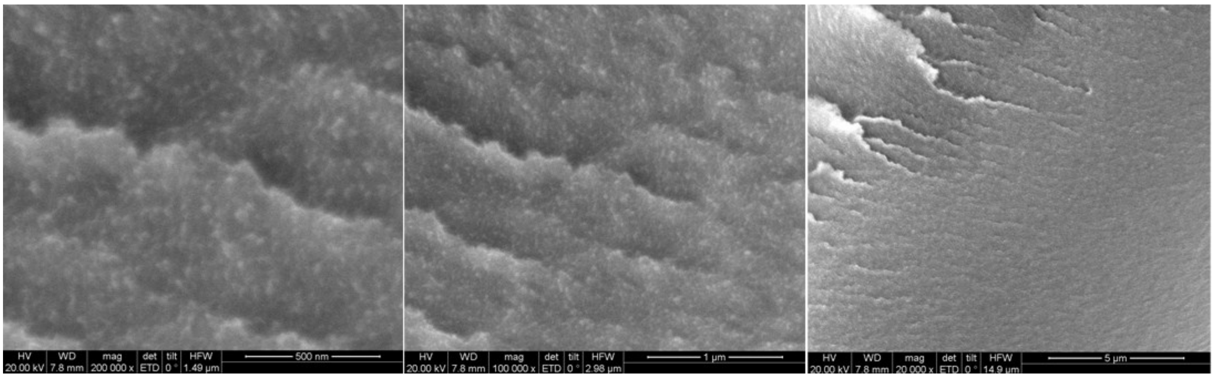

Figure S10. SEM images of xerogel at different magnification times (500 nm, 1μm, and 5μm), no pore structure could be observed.

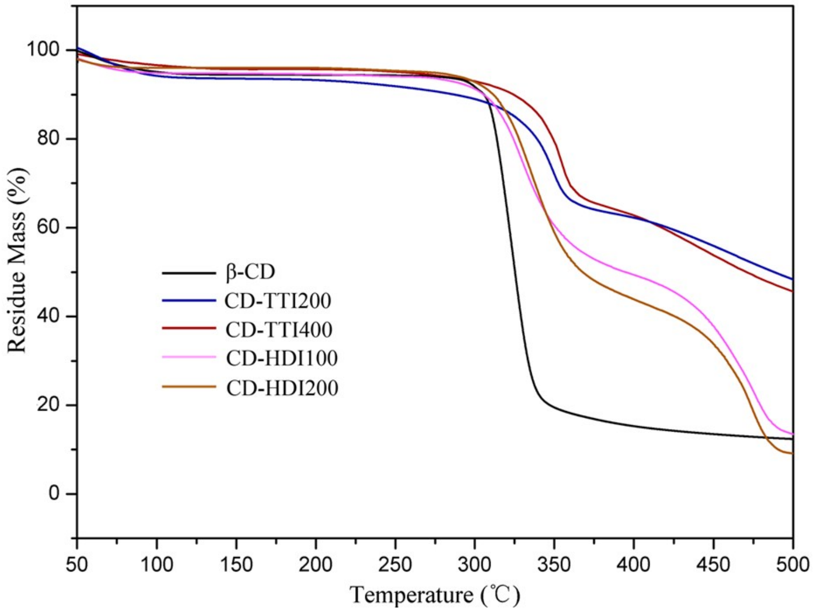

Figure S11. TG traces of the selected aerogels and β-CD.

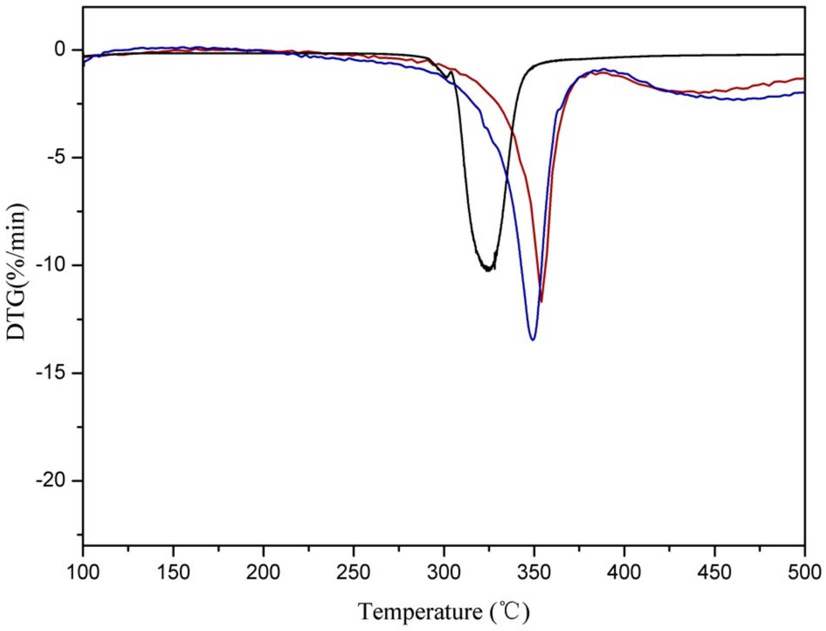

Figure S12. DTG curves of β-CD (black), CD-HDI200 (blue) and CD-TTI200 (red) at a heating rate of 10 °C/min.

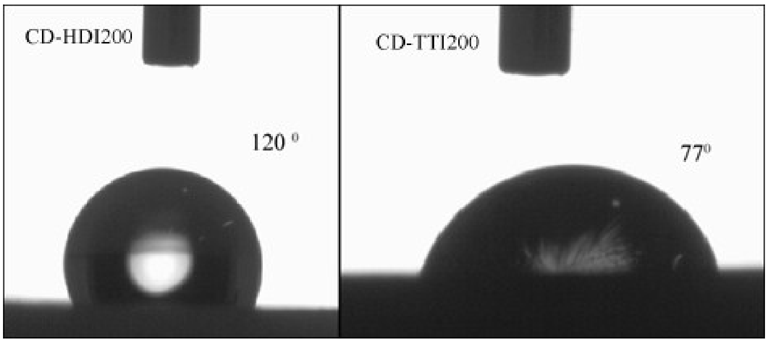

Figure S13. Contact angle measurement of CD-HDI200 and CD-TTI200.

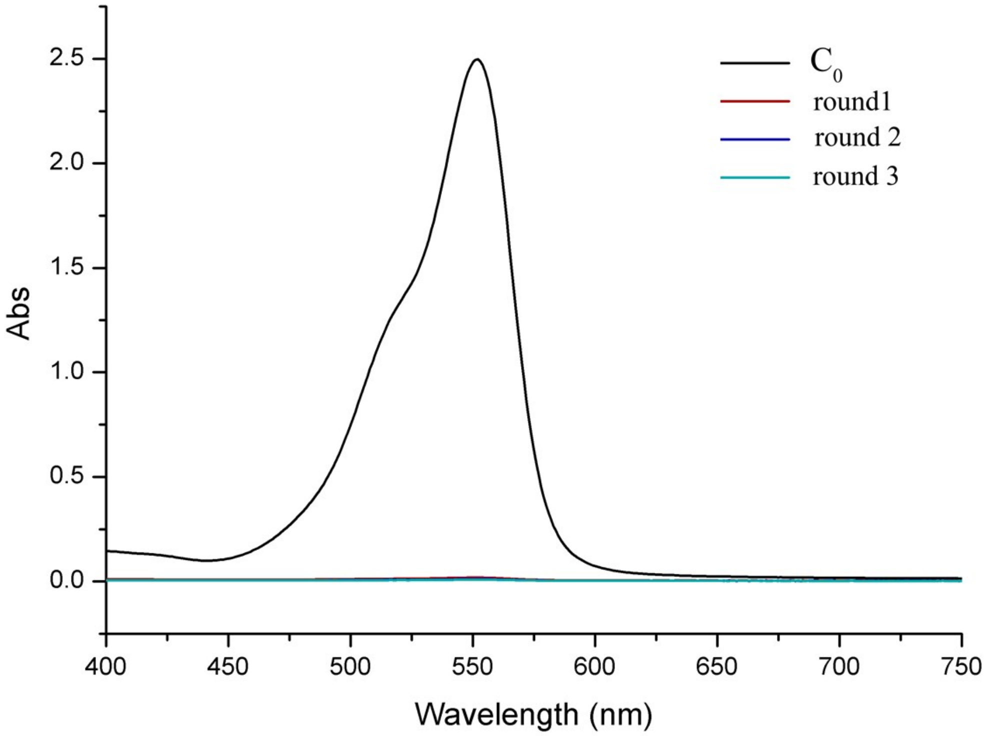

Figure S14. UV-vis spectra of rhodamine B aqueous solution (0.075 mM) and the solution after adsorption and reused by washing with methanol. The solution been used was 8 ml, and the adsorbent is 4 mg.

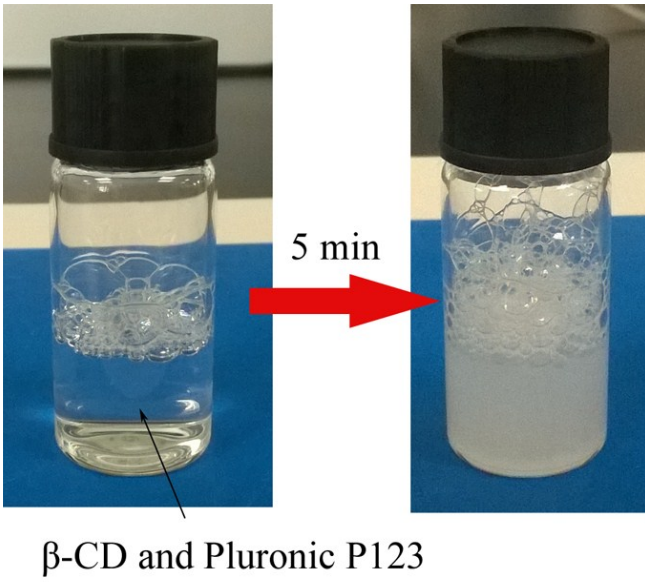

Figure S15. Photo image of the self-assembly of CD and Pluronic P123

Figure 13 indicate the self-assembly of β-CDs and Pluronic P123. The photo image shows the mixture of saturated β-CDs aqueous solution and Pluronic P123, which is a clear solution upon mixing. However, after 5 min, the solution became opaque, which indicate the assembly between β-CDs and Pluronic P123 happened. β-CDs can selectively include the PPO segment of Pluronic P123, forming a channel-type crystalline structure, and result in the precipitate.[1-3]

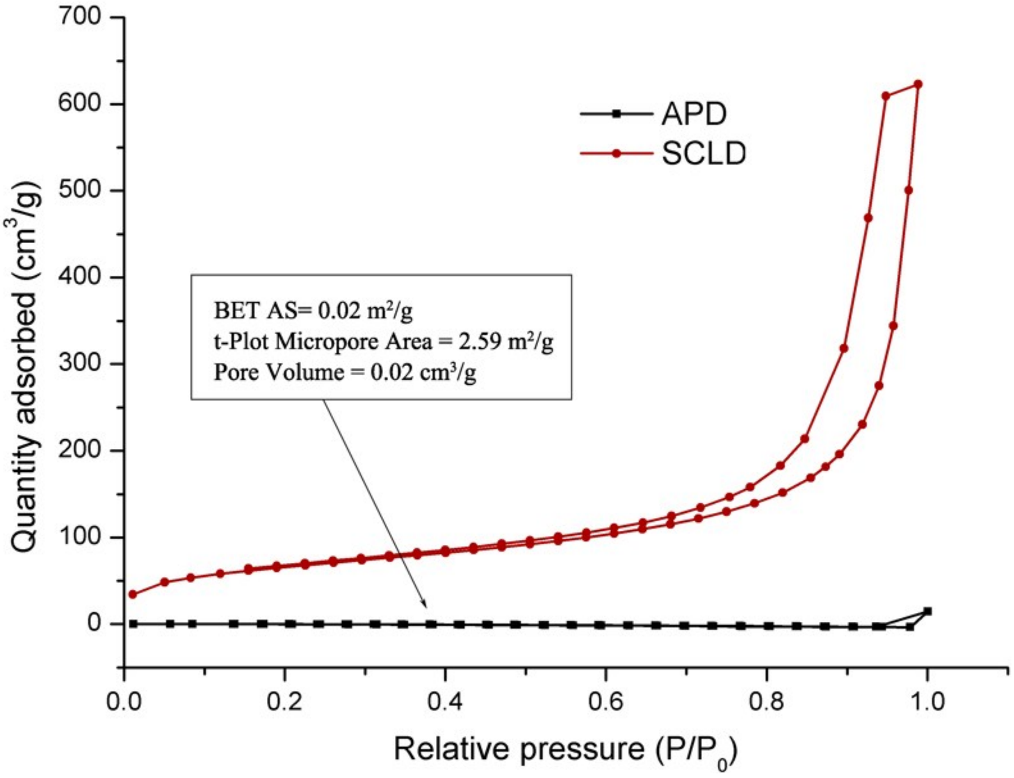

Figure S16. N_2 adsorption-desorption isotherms of the aerogel CD-TTI200 dried by APD and SCLD.

Gels dried via SCLD possess a high BET SA of 233 m^2/g as shown in Table 1 (233/0.02=11650 times to the APD sample). However, gels dried at ambient pressure (APD) remarkably shrinking with all most no SA as presented in Figure S14. Moreover, the pore volume of the sample prepared by APD could be ignored (0.96/0.02=48 times). Interestingly, the APD dried samples possess a micropore surface of 2.59 m^2/g, possibly due to the CDs cross-linked by rigid TTI.

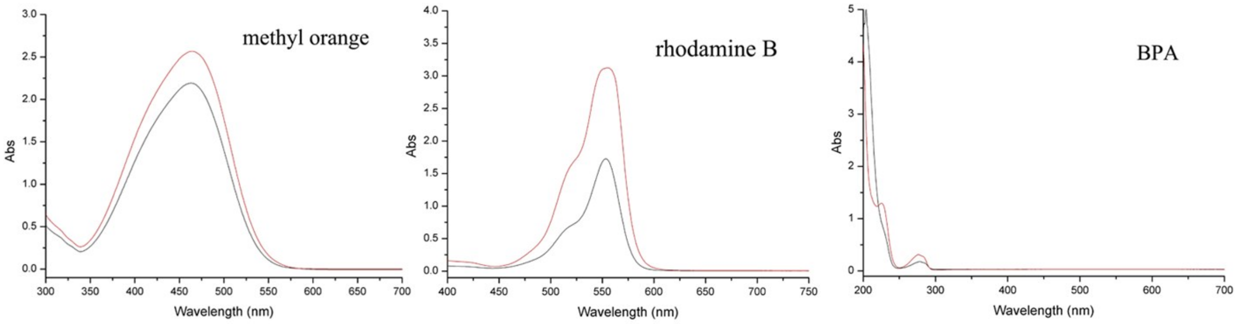

Figure S17. UV-vis spectra of the solution before (red line) and after adsorption (black line), the absorbent is the xerogel, original concentration of the solution is 0.1 mM.

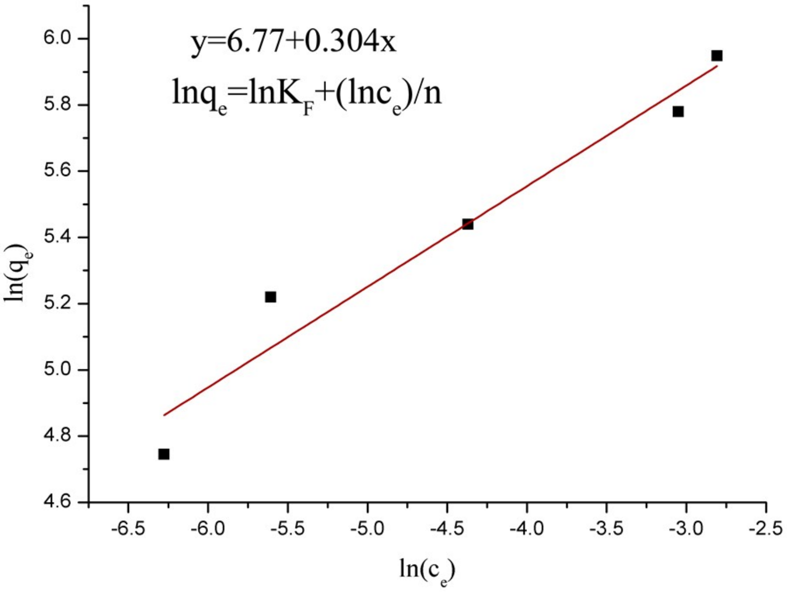

Figure S18. Adsorption isotherm fits the Reundlich model for the adsorption of rhodamine B by CD-TTI200.

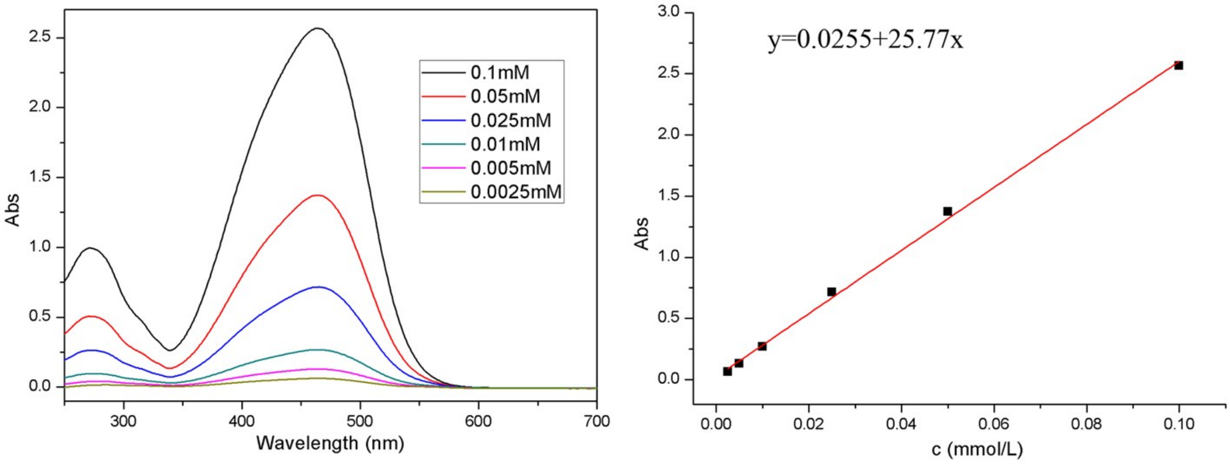

Figure S19. UV-vis spectra of methyl orange at difference concentration (left) and their pseudo-second-order plot (right).

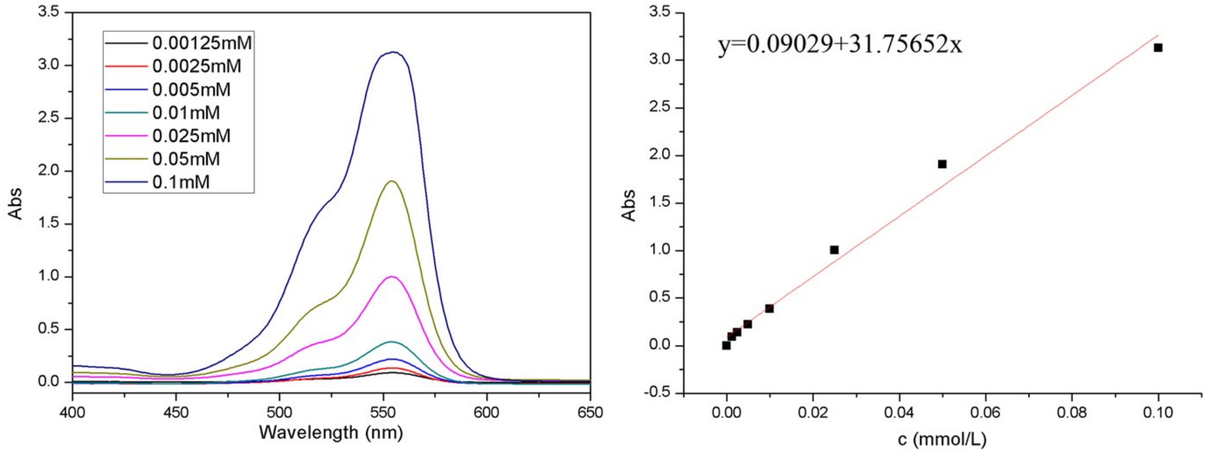

Figure S20. UV-vis spectra of rhodamine B at difference concentration (left) and their pseudo-second-order plot (right).

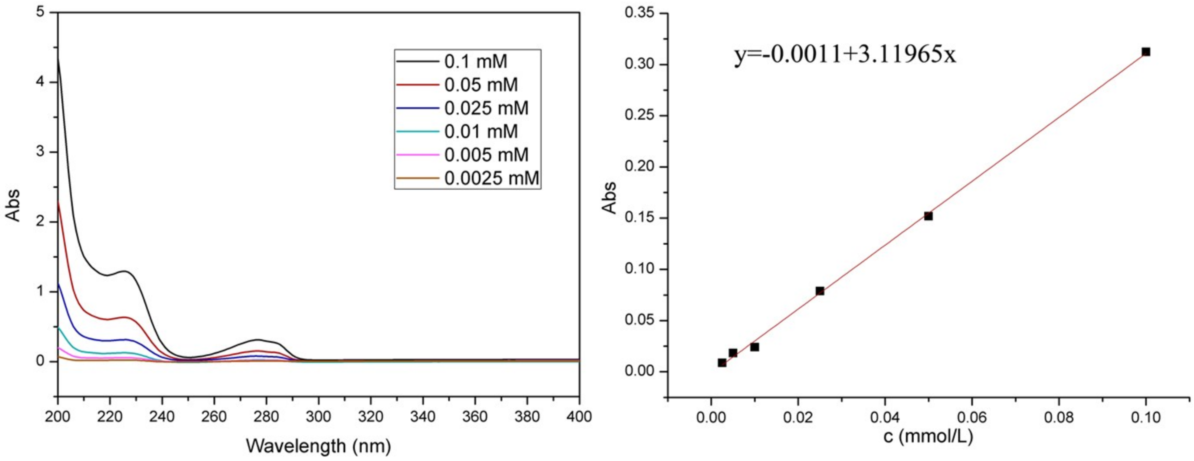

Figure S21. UV-vis spectra of Bisphenol A at difference concentration (left) and their pseudo-second-order plot (right).

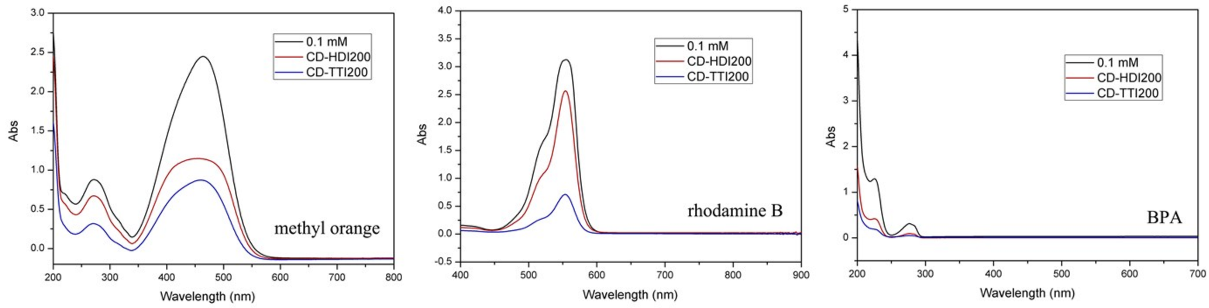

Figure S22. UV-vis spectra of the solution before and after adsorption.

Reference:

1. J. Wang, L. Ye, A. Zhang, Z. G. Feng, *J. Mater. Chem.* **2011**, 21, 3243.
2. A. Harada, J. Li, S. Suzuki, M. Okada, M. Kamachi, *Macromolecules* **1993**, 26, 5267.
3. J. Wang, P. Gao, L. Ye, A. Zhang, Z. G. Feng, *J. Phys. Chem. B* **2010**, 114, 5352.